Ablating Cones," *Journal of Spacecraft and Rockets*, Vol. 8, No. 2, Feb. 1971, pp. 161–169.

[3] Nachtsheim, P. R., "Analysis of the Stability of a Thin Liquid Film Adjacent to a High-Speed Gas Stream," TN D-4976, 1969, NASA.

[4] Nachtsheim, P. R. and Hagen, J. R., "Observations of Crosshatched Wave Patterns in Liquid Films," AIAA Paper 71-622, Palo Alto, Calif., 1971.

[5] Moore, F. K., "Laminar Boundary Layer on a Circular Cone in Supersonic Flow at a Small Angle of Attack," TN 2521, 1951, NACA.

[6] Moore, F. K., "Displacement Effect of a Three-Dimensional Boundary Layer," TN 2722, 1952, NACA.

[7] Sedney, R., "Laminar Boundary Layer on a Spinning Cone at Small Angle of Attack in a Supersonic Flow," *Journal of the Aeronautical Sciences*, Vol. 24, No. 6, June 1957, pp. 430–436.

[8] Martin, J. C., "On Magnus Effects Caused by the Boundary-Layer Displacement Thickness on Bodies of Revolution at Small Angles of Attack," *Journal of the Aeronautical Sciences*, Vol. 24, No. 6, June 1957, pp. 421–429.

APRIL 1973 AIAA JOURNAL VOL. 11, NO. 4

Ballistic Range Investigation of Sonic-Boom Overpressures in Water

PETER F. INTRIERI* AND GERALD N. MALCOLM†
NASA Ames Research Center, Moffett Field, Calif.

An investigation of sonic-boom overpressures in water has been conducted in the Ames Research Center Pressurized Ballistic Range by gun-launching small cone-cylinder models over water. Flights were conducted at Mach numbers of 2.7 and 5.7 in air, corresponding to Mach numbers of 0.6 and 1.3, respectively, in water. Shadowgraph pictures and underwater pressure measurements indicate that for horizontal flights at Mach numbers below Mach 4.4 in air (i.e., subsonic Mach numbers relative to the speed of sound in water) the resulting underwater disturbance is an acoustic wave whose peak pressure attenuates rapidly with water depth. Comparison of experimental data for the subsonic case with existing theoretical predictions of attenuation with depth shows good agreement. In contrast, at supersonic Mach numbers, relative to water, the incident shock wave at the surface is transmitted into the water as a propagating shock wave and the peak pressure associated with it is not affected by water depth but attenuates as it does in air.

Nomenclature

a = speed of sound
h = distance from flight path to pressure cell
h_w = distance from flight path to water surface
l = model reference length
M = Mach number
Δp = overpressure or pressure change from ambient pressure
Δp_o = overpressure at water surface behind reflected incident shock wave
Δp_{max} = maximum or peak overpressure from ambient pressure
t = time
T = period of N-wave
V = velocity of incident shock wave in air parallel to water surface (also velocity of model in flight)
ζ = normalized depth parameter [see Eq. (1)]
θ = angle of incidence between incident shock wave and water surface
θ_c = critical angle of incidence
μ = Mach angle, $\sin^{-1} 1/M$
τ = normalized time parameter, t/T

Presented as Paper 72-657 at the AIAA 5th Fluid and Plasma Dynamics Conference, Boston, Mass., June 26–28, 1972; submitted July 2, 1972; revision received November 15, 1972. The authors thank R. Hicks and J. Mendoza of Ames Research Center for bringing to our attention the apparent need for underwater sonic boom tests, and M. Wilkins, for his assistance in obtaining the shadowgraph pictures and performing the fish experiments.

Index categories: Aerodynamic and Powerplant Noise (Including Sonic Boom); Atmospheric, Space, and Oceanographic Sciences; Undersea Acoustics.

* Research Scientist.

† Research Scientist. Member AIAA.

Introduction

THERE is a great deal of concern about the effects of sonic-boom overpressures over land and populated areas. There has been less concern about overpressures that occur over water and the resulting underwater pressure disturbances. It is important to understand these disturbances since they may have significant underwater environmental effects. To date, a few theoretical and experimental studies concerning underwater pressures induced by sonic booms have been conducted. Sawyers[1] and Cook,[2] for example, have developed similar theories for the case of a planar N-wave traveling horizontally over a smooth water surface at a constant speed less than the speed of sound in water ($M_{air} < 4.4$). Their results indicate that the incident shock wave at the air-water interface is totally reflected and the pressure disturbance at the surface penetrates into the water as sound waves. Furthermore, the sound pressure is shown to attenuate rapidly with both increasing frequency and depth in the water. To test the validity of these theories, Waters and Glass[3] conducted experiments using air blasts from explosive charges over a water surface (flooded quarry, 90 m wide and 24 m deep) to produce shock waves simulating a sonic boom. Pressure measurements were made underwater at various depths and their results showed good agreement with Sawyers' theory.[1] Conversely, Urich,[4] using minimal data obtained from a few aircraft flights over the ocean and hydrophones submerged at various depths, concludes that peak pressures fall off more rapidly with depth than predicted and therefore the existing theories are not valid. The only explanation offered for the discrepancy was a possible effect from wave scattering due to a rough sea surface. Thus, from the literature, it appears that additional work concerning sonic-boom effects underwater is warranted even for the

case where the air speed is less than the speed of sound in water.

An area of concern for which no experimental data have been obtained and the one that provided the initial impetus for conducting the present experimental investigation is the case of underwater effects from flights at speeds *greater* than the speed of sound in water. References 2 and 3 indicate that for this condition the incident shock wave should not be totally reflected at the surface and that a shock wave rather than sound waves will be produced underwater. To the authors' knowledge, no experiments are reported in the literature to specifically investigate a sonic-boom-induced underwater shock wave and in particular to determine its variation in strength with depth in the water.

The present experiments were designed to determine these effects by measuring pressures underwater produced from flights of small gun-launched models over a water surface in a ballistic range. Models were flown at speeds both less than and greater than the speed of sound in water. Experimental results from these two regimes are presented and, where possible, compared to existing theory. The pressure results are supplemented by shadowgraph pictures that show the shock-wave systems both in air and underwater.

Tests and Instrumentation

To save time and reduce costs it was desirable to make effective use of existing facilities and instrumentation where possible. For these reasons, the Ames Pressurized Ballistic Range was chosen as a suitable facility. This facility is used primarily for studying the aerodynamic characteristics of gun-launched free-flight models. It is 61.8 m (203 ft) long, 3.05 m (10 ft) in diameter, and contains 24 orthogonal shadowgraph stations. An open-top plexiglass tank containing water was positioned on the floor between shadowgraph stations for the purpose of taking underwater pressure measurements, and a second, smaller tank was placed directly in a shadowgraph station to obtain the desired shadowgraph pictures. Both tanks were positioned directly under the flight path of the projectile. Figure 1 is a sketch of the test setup.

The tests were conducted at ambient conditions of pressure and temperature at Mach numbers 2.7 and 5.7 in air or Mach numbers 0.6 and 1.3, respectively, relative to the speed of sound in water. A 12.7-mm-diam (0.5 in.) powder-gas gun was used to launch the models—steel 45° half-angle cone-cylinders, 1.19 cm long and 1.25 cm in diameter. A sketch of the large plexiglass tank used for underwater pressure measurements is presented in Fig. 2. This tank and the flat plate shown with the pressure cell could be moved independently in a vertical direction to vary the distance from the flight path. The water level could also be adjusted to vary the depth of the pressure cell beneath the surface. A 0.56-cm-diam quartz pressure transducer (Kistler model 603A),

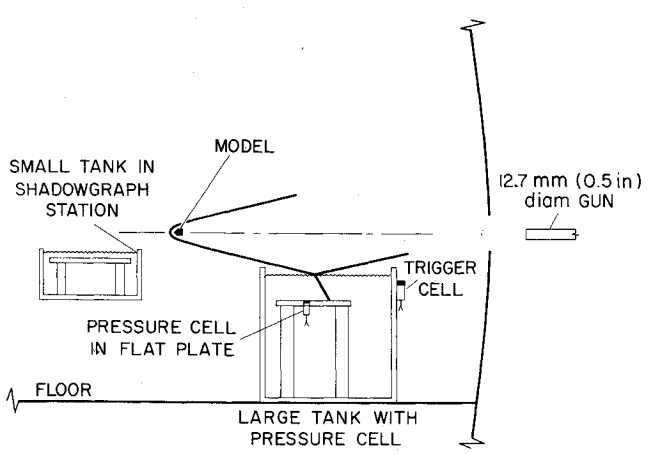

Fig. 1 Sketch of test setup in ballistic range.

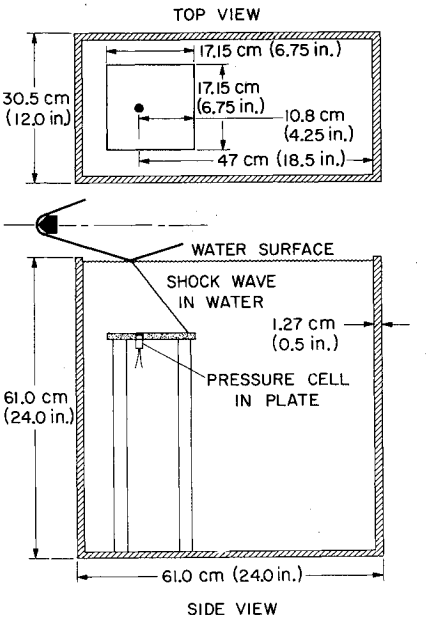

Fig. 2 Dimensional sketch of large plexiglass tank with pressure transducer.

having a nearly flat frequency response from d.c. to its resonant frequency of approximately 400 kHz was flush-mounted in silicon rubber compound in a 1.27-cm-thick aluminum plate approximately 17 cm square. A waterproof microdot cable connected the pressure cell to a Kistler model 566 electrostatic charge amplifier, the output of which was displayed on an oscilloscope and photographically recorded. Oscilloscope sweep was triggered by another transducer placed outside the tank in such a position that it sensed the shock wave a short length of time before arrival at the recording cell. The small plexiglass tank (30.5 cm × 15.25 cm × 15.25 cm deep) placed in the shadowgraph field of view also contains a submerged plate so as to duplicate the underwater shock-wave reflection expected in the large tank.

A few tests were also conducted with the pressure transducer alone, i.e., without a flat plate surrounding it. This technique yielded results similar to those reported here but was judged less desirable since the relatively small reflecting surface (i.e., the 0.56-cm-diam face of the cell itself) caused sizable edge effects to be introduced into the pressure records. A discussion of these cell-alone data is presented in Ref. 5 for the interested reader. In addition, a few exploratory tests were also conducted to determine any gross effects of underwater shock waves on small fish (guppies). The present fish experiments (conducted at supersonic speeds relative to water) were motivated by the work (at subsonic speeds) reported in Ref. 6, which concluded, as did the present study, that no detrimental effects were observed. Of course, whether this result would also occur for sonic booms of longer duration such as those associated with full-scale flight or whether there are long-term biological effects is not known.

Results and Discussion

The results from these experiments consist of two types of data —shadowgraph pictures and underwater pressure measurements. The two principal flight regimes studied were at subsonic speeds ($M_{water} = 0.6$) and supersonic speeds ($M_{water} = 1.3$) with respect to the speed of sound in water. Shadowgraph pictures will be presented first, followed by examples of the pressure signatures measured underwater at various depths. Where possible, pressure measurements will be compared with theory.

Shadowgraph Pictures

Figure 3 is a shadowgraph picture taken with a conical light system, of a model flying over the small plexiglass tank containing

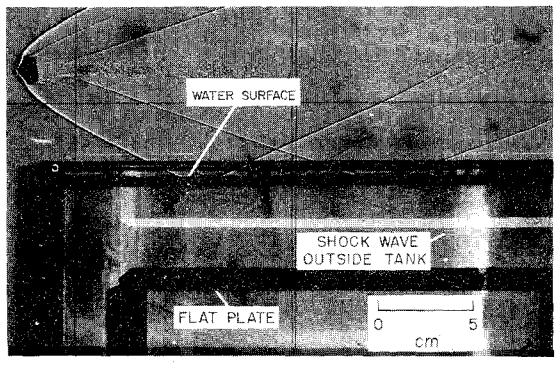

Fig. 3 Shadowgraph picture of model flying over plexiglass water-filled tank at Mach 2.7 in air ($M_{water} = 0.6$).

water. As noted, a flat plate is submerged beneath the surface to duplicate the arrangement in the larger tank containing the pressure transducer. To enhance the readers' interpretation of this picture and following ones, some comments are in order about the effects of the conical light system on the shadowgraph pictures. The film is exposed by a point-source light, a high-intensity short-duration spark, thereby producing conical light rays that give the picture a pseudo-three-dimensional appearance. In Fig. 3 the two narrow bands at the top of the tank are the top edges of the near and far sides of the tank looking across the 15.25-cm width. The third dark band is the surface of the water (note that the light strikes the water surface below the critical angle for transmission). The lighter bands are reflections of light from the submerged flat plate and tank edges. The shadow of the plate is easily discernible. The model is flying at $M = 2.7$ or subsonic ($M_{water} = 0.6$) relative to the speed of sound in water. The incident shock wave is seen to reflect from the water surface and, as expected, no underwater shock wave can be seen. (Shock waves that appear to be in the tank at the same angle as the wave in air are actually outside the tank on either side.) The underwater disturbances that do occur in this case are discussed in a later section of pressure measurements.

Figures 4a and b are shadowgraph pictures of a model in flight over the water tank at $M = 5.7$ or supersonic ($M_{water} = 1.3$) with respect to the speed of sound in water. The underwater shock wave resulting from the impingement of the projectile bow wave on the water surface is readily seen. The shock wave produced in water by the trailing shock is apparently too weak to be visible by the shadowgraph system although evidence of its existence, at least at shallow depths, will be seen subsequently in the pressure records. The shock waves in water are at an angle of approximately 52° with respect to the plate. Note that this angle for the underwater shock wave corresponds to a Mach angle, μ, for $M = 1.3$ ($\mu = \sin^{-1} 1/M$), which is consistent with the Mach number calculated from the speed of sound of water.

As noted in Fig. 4a, the submerged plate is aluminum and the shock wave in water reflects from the top surface. As shown in Fig. 4b and discovered quite by accident, the underwater shock wave passes through a plexiglass plate almost undisturbed. This unimpeded transmission of the shock wave through plexiglass occurs because the acoustic impedance (defined as the product of the density and the speed of sound) of water and plexiglass are nearly identical. The acoustic impedance of aluminum is much greater than water, thus the wave is reflected in that case.

Pressure Measurements

The behavior of the shock-wave system in the shadowgraph picture with the aluminum plate (Fig. 4a) is similar to the shock-wave system present in the larger plexiglass tank used for measuring pressures. The principal parameter of interest in these experiments is the peak pressure associated with the leading shock wave both in air and under water and particularly its variation with depth. The measured peak pressures are determined from the oscilloscope record of the pressure signature (signatures typically have a characteristic N-shape). As noted in the description of test equipment, the pressure cell is flush-mounted in a flat plate. Because pressure disturbances are reflected at the surface of the cell and plate, the recorded pressure measurements have a built-in reflection factor. For the present experiments, the shock strengths are such that the reflection factor is very near 2 (for strong shocks, the reflection factor can be greater than 2). Therefore, all recorded pressures are essentially double the pressures that would be measured directly. Before examining some sample pressure records, the method used to vary the water depth and the nature of the shock-wave system at the surface should be discussed.

The shock wave emanating from a projectile in flight approaches a conical shape, i.e., the Mach cone. The shock angle will be very nearly equal to the Mach angle at only a few body diameters from the flight path. The intersection of this Mach cone with a plane surface parallel to the flight path forms a hyperbola whose vertex advances over the surface with the speed of the projectile. For full-scale flights (at sufficient altitude), the radius of curvature of the hyperbola at the vertex is large in comparison to the length of the N-wave and the depths of water of interest. For this case, the shock wave impinging on the surface can be considered a planar incident wave. (This is the assumption used in Refs. 1 and 2, where the theory for predicting the behavior of sonic-boom overpressures underwater was developed.) For the present experiments, since measurements are made relatively close to the flight path, the ratios of the radius of curvature of the hyperbola to N-wave length and to water depth are not large enough for this assumption to be strictly valid. However, as shown later, violating this assumption has little effect on the results. When the radius of the hyperbola is small as it is for the present experiments, one does not have to move very far to the side of the flight path before the Mach number normal to the hyperbola begins to decrease from the flight Mach number. (It approaches Mach 1 if one moves far enough.) However, if measurements are made directly under the flight path, the recorded

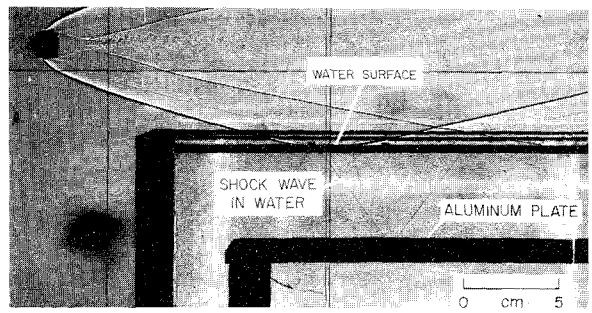

a) Tank contains submerged aluminum plate

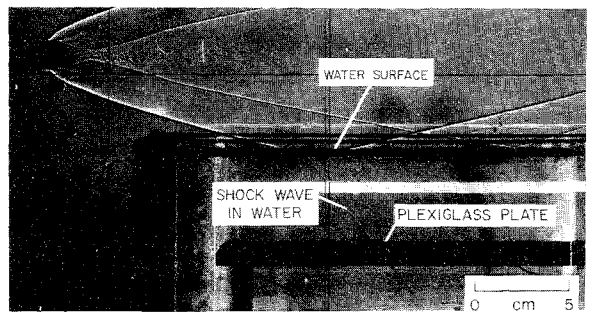

b) Tank contains submerged plexiglass plate

Fig. 4 Shadowgraph pictures of model flying over plexiglass water-filled tank at Mach 5.7 in air ($M_{water} = 1.3$).

pressure signature will be the one corresponding to the flight Mach number and not a lower one.

One other consideration was made during the tests. Since measurements were made near the flight path where the shock shape cannot be considered planar but approaches a Mach cone, the magnitude of the pressure jump across the bow shock wave decreases as distance from the flight path is increased. For low Mach numbers ($M < 3$), this variation with distance can be predicted rather well by theoretical methods[7] that have been verified extensively by experiments. When the present experiments were initiated, it was reasoned that this effect could be minimized by keeping the distance between the pressure transducer and the model flight path as constant as possible (there are some slight variations because the flight-path location varies from test to test). To increase water depth, the water level was raised in the tank above the stationary transducer. This, of course, introduces another problem because the water surface is now closer to the flight path and there is now a higher pressure at the surface. This method, nevertheless, was judged preferable to moving the transducer with respect to the flight path and keeping the water level a constant distance from the flight path. (If one could take measurements where the depth in water is small compared to the distance of the water surface from the flight path, such as typical full-scale flights at high altitudes, then the pressure change due to moving away from the flight path is insignificant due to that caused by water depth.) The present method of varying depth does not eliminate all the problems associated with measurements taken close to the flight path but can be shown to be a reasonable approach as will be discussed further when the results are compared to theory.

With this procedure in mind, see Fig. 5 where examples of pressure records obtained from the plate-mounted pressure cell at both supersonic and subsonic conditions in water are shown. The four signatures on the left were obtained with the model flying at $M = 5.7$ in air, or $M = 1.3$ in water, whereas those on the right are for a model traveling at $M = 2.7$ in air or $M = 0.6$ in water. This figure shows significant differences in the pressure records between the supersonic and subsonic cases as the water depth changes. The records for the subsonic case show rapid decay in strength and a rounding off (loss of high-frequency content) of the signature with water depth. In contrast, for the supersonic case, there is little variation in peak pressure with water depth; the records just appear to be less smooth. The

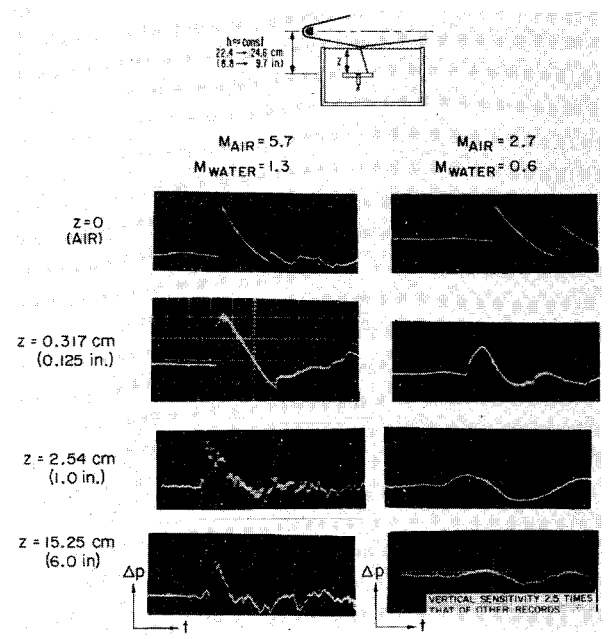

Fig 5 Sample oscilloscope records of pressure measurements in air and underwater.

characteristic N-shaped wave can be discerned, however, even at a depth of 15 cm. Clearly, the differences in underwater propagation of acoustic and shock waves are well represented by these records. Pressure data associated with each of these two speed regimes, subsonic and supersonic, will be examined in detail and comparison with theory will be made.

Review of Underwater Acoustic Theory

Since theoretical methods are available for predicting the attenuation of underwater sound waves with depth, comparisons can be made with the present experimental results. First, however, it will be helpful to briefly describe the theoretical techniques that exist. One technique to be considered assumes a plane sinusoidal acoustic wave. While this is useful in roughly estimating pressure attenuation with depth, it is not truly applicable to the wavefront associated with a sonic boom which is normally some variation of a classic N-wave and is equivalent to sinusoidal waves of many frequencies superimposed on one another. Therefore, the more sophisticated approaches using plane N-waves that have been developed will be reviewed. The effects of viscosity on attenuation rate is also briefly reviewed.

Plane sinusoidal wave

The theory of the reflection, transmission, and penetration of a plane sinusoidal wave (single frequency) at a smooth air-water interface is described in Ref. 8 and referred to in Refs. 3 and 4. A plane wave is assumed to propagate in the direction of the normal to the wavefront at the speed of sound in air. The critical angle for transmission of energy across the air-water interface, θ_c, measured as the angle between the acoustic wavefront and the water surface, is approximately 13°, [$\theta_c = \sin^{-1}(a_{air}/a_{water})$, where a_{air} and a_{water} are the speeds of sound in air and water, respectively]. For angles of incidence less than this, the acoustic wave moves parallel to the surface of the water at a speed greater than the speed of sound in water and acoustic energy from the wavefront is partially reflected from the surface and partially transmitted into the water in the form of a homogeneous propagating acoustic wavefront (i.e., a shock wave). However, for waves whose angles of incidence is greater than 13° and consequently whose rate of travel parallel to the surface is *less* than the speed of sound in water, there is total reflection of the incident wavefront and only sound waves penetrate the water. The amplitude of this penetrating sound pressure, Δp, normalized by the initial overpressure just beneath the surface, Δp_o, decays exponentially with depth and frequency.

Plane N-waves

Theoretical methods for predicting the underwater pressure signature of a plane N-wave sweeping across a water surface have been developed by both Sawyers[1] and Cook[2] and corroborated with experimental data by Waters and Glass.[3] (The theories of Sawyers and Cook are nearly identical. Cook has an additional term in his expression for the underwater waveform but it has a negligible contribution to the over-all sound pressure.) Both theories use a Fourier transform approach to characterize the N-wave (the details can be found in Refs. 1 and 2). The results can be summarized as follows. The time-varying waveform or pressure signature that would be sensed at a fixed location under water at various depths, z, can be expressed as[1,3]

$$\Delta p(z,t)/\Delta p_o = (\zeta/\pi)\Big[\{(\tau/\zeta)+[(\tau-1)/\zeta]\}\times \{\arctan[(\tau-1)/\zeta]-\arctan(\tau/\zeta)\}+ (\ln[1+(\tau/\zeta)^2]-\ln\{1+[(\tau-1)/\zeta]^2\})\Big] \quad (1)$$

where Δp_o is the pressure at the surface or zero depth, $\tau = t/T$ is a normalized time variable, and $\zeta = [1-(V^2/a^2_{water})]^{1/2} \times z/VT$ is a normalized depth variable where V is the velocity of the N-wave front parallel to the water surface at zero depth, z is depth, and T is the period of the N-wave at the surface.

Equation (1) can be used to calculate $\Delta p/\Delta p_o$ as a function of τ at various values of ζ. Examples of calculated pressure signatures, $\Delta p/\Delta p_o(\tau)$ are shown in Fig. 6, where the ζ values

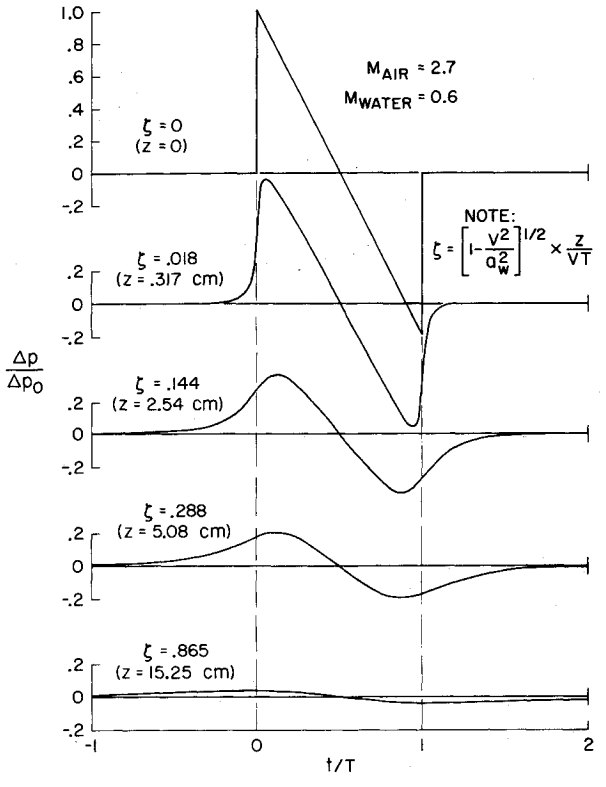

Fig. 6 Calculated pressure signatures at various depths in water using theory of Ref. 1.

selected are those resulting from the z locations used in the present experiments. For the purpose of calculating ζ from the experimental z locations, the following values were used for the parameters contained in ζ: T was taken as the period of the N-wave at the surface, which was 0.150 msec, $V = M_{\text{air}} \times a_{\text{air}} = 2.7 \times 341$ m/sec $= 920$ m/sec, and $a_{\text{water}} = 1490$ m/sec.

The calculated pressure signatures plainly illustrate the change in shape (significant loss of high frequencies as we would expect) and reduction in pressure level as ζ is increased. These signatures show good qualitative agreement with those shown earlier in Fig. 5. The peak pressure from each of these calculated signatures plus others at additional ζ values can be plotted vs their respective ζ values and a curve faired through the points. The result is a plot of the variation in peak pressure with the normalized depth parameter, ζ, as shown by the curve plotted in Fig. 7. Note that if the decay in pressure with depth were exponential, as it is for a single-frequency sinusoidal wave, this curve would be a straight line, and it obviously is not. Discussion of the plotted data points will follow later.

Pressure losses due to viscosity

One additional source of sound pressure attenuation was examined to put it in its proper perspective. Effects of viscosity were calculated from an expression in Ref. 9. It was found that even for frequencies as high as 1 MHz, the viscosity losses can be considered negligible. For frequencies pertinent to full-scale sonic booms (<100 Hz), viscosity effects are essentially nonexistent regardless of depth.

Comparison of Subsonic Underwater Pressure Data to Acoustic Theory

Pressure data obtained for the Mach 2.7 flights are plotted in Fig. 7 for comparison to the theoretical curve already discussed. (Error bars represent the uncertainty in measuring the peak pressure from the oscilloscope traces.) Some comments about the experimental data are in order at this point. Since the incident wave is totally reflected at the surface and the reflected wave has the same strength as the incident wave, the measured pressure just below the interface is essentially double that behind the incident wave just above the surface. This doubling effect was discussed earlier with regard to measurements on a flat plate and is also applicable to the smooth air-water interface, since calculations indicate the deflection of the water surface by the incident wave is negligible. It is this "doubled" pressure that is used as the reference surface pressure, Δp_o.

In describing the method for varying water depth, it was stated that the distance between model location and the pressure transducer was held constant while the water depth was varied by increasing the water level above the transducer. This necessarily results in moving the water surface closer to the flight path with increasing depth. Because there are geometric effects on the incident shock strength, the closer one moves to the flight path the greater the pressure will be behind the incident shock wave. This means that the reference pressure, Δp_0, increases as the water depth, z, increases. The need for this information was not apparent when the tests were made; hence, pressure measurements in air were made at only one location from the flight path and, therefore, no experimental values for surface pressure were determined at the other locations. However, they can be estimated by the following procedure. At Mach numbers of 3 or less for shock strengths encountered in the present tests, it has generally been found experimentally and predicted theoretically[7] that the pressure behind the incident shock wave at several body diameters from the flight path decreases inversely with the $\frac{3}{4}$-power of the distance from the flight path, i.e.,

$$\Delta p_o = k/(h_w)^{3/4} \tag{2}$$

where k (for these experiments) can be determined from the one measured pressure of 0.194 atm at $h_w = 23.46$ cm, $k = (0.194)(23.46)^{3/4} = 2.073$. With Eq. (2) the surface pressures at any other location from the flight path can be calculated. For comparison to theory, the underwater peak pressure, $\Delta p_{\max}$, measured at various z locations was normalized by the calculated reference pressure, Δp_o, appropriate for that point. These calculated values and the ratios plotted in Fig. 7 are shown in Table 1. The agreement with the theoretical curve is considered quite good. Results from present experiments and those of Waters and Glass[3] both support the theory even though they were conducted with completely different techniques and greatly differing time scales; i.e., for the present experiments the duration of the N-wave was typically 0.150 msec and for the Waters and Glass experiments the duration was approximately 1.5 msec. It should also be noted

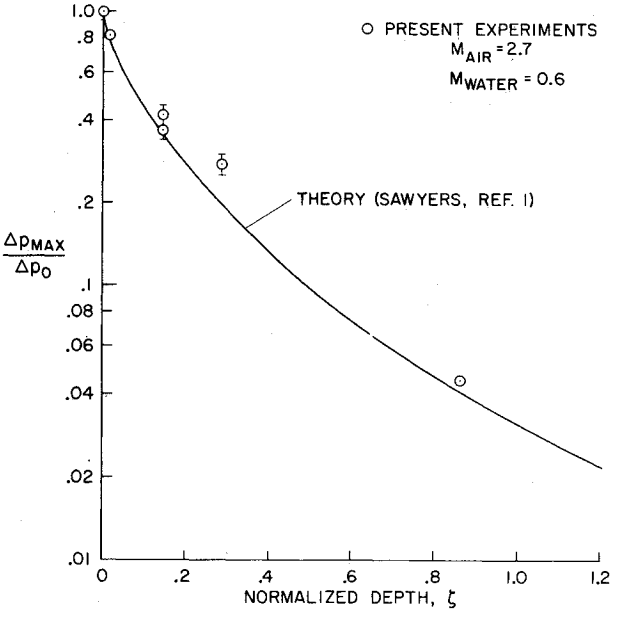

Fig. 7 Variation of peak pressure from underwater sound waves with normalized depth parameter.

Table 1 Subsonic test results

Test	z, cm	h, cm	h_w, cm	Δp_{max}, atm	Δp_o, atm	$\frac{\Delta p_{max}}{\Delta p_o}$	ζ
1	0.0	23.46	23.46	0.194	0.194	1.000	0.0
2	0.32	24.02	23.70	0.158	0.192	0.821	0.002
3	2.54	23.61	21.07	0.088	0.210	0.420	0.144
4	2.54	23.79	21.25	0.078	0.210	0.373	0.144
5	5.08	23.79	18.71	0.064	0.230	0.278	0.288
6	15.25	24.89	9.64	0.017	0.379	0.045	0.865

that the pressure levels for the present experiments were approximately two orders of magnitude higher than those in the Waters and Glass experiments and those normally found for full-scale aircraft flights. These results, together with the following additional considerations—1) the theory, supported by both the present experimental results and those of Waters and Glass, is based on pressure and wave-duration parameters that have been normalized and is therefore independent of absolute values of pressure and time, and 2) the shock wave from full-scale flight at altitude would be an even closer representation of the planar wave assumption of the theory than the shock wave produced in the present experiments—infer that the theory might be applicable to full-scale N-waves that are typically on the order of 100–300 msec duration. As noted earlier, however, the theory assumes a smooth water surface and any irregularity such as wave action may affect the actual underwater pressure disturbance. The application of the theory to full-scale flight should be verified by flight experiments involving aircraft over water.

Supersonic Underwater Pressure Data

Consider now the case where the model is traveling at $M = 5.7$ or greater than the speed of sound in water. As noted in Fig. 4, a shock wave is formed and the example pressure signatures in Fig. 5 showed essentially no loss in peak pressure due to water depth. In Fig. 8 the underwater peak pressure has been plotted as a function of water depth with the distance from flight path to pressure transducer held essentially constant. The error bars represent the variations from test to test and the uncertainty in reading the oscilloscope records. As noted in the sample pressure traces, there is essentially no decay of the peak pressure with depth. As pointed out earlier for the $M = 2.7$ tests, moving the water surface closer to the flight path increases the magnitude of the pressure disturbance at the surface. However, as is evident here, the pressure that exists at the transducer is the same in each case. This means that the peak pressure drops from its value

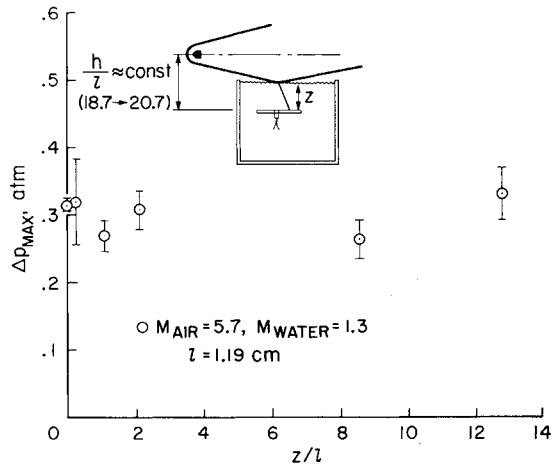

Fig. 8 Variation of peak pressure with water depth using pressure cell mounted in flat aluminum plate.

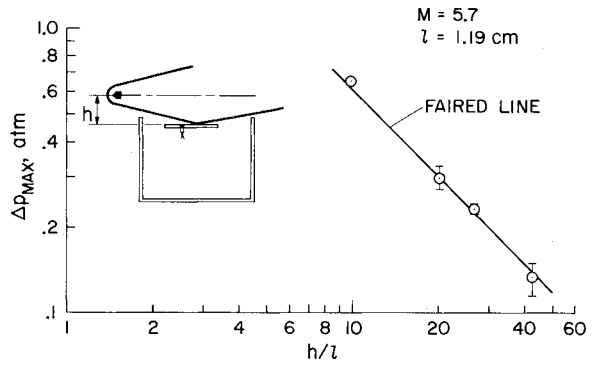

Fig. 9 Variation of peak pressure in air with distance from flight path.

at the surface to a value that is solely dependent on the distance of the transducer from the flight path. This behavior implies that the presence of water is of little consequence. In principle, if one had a planar shock wave at the surface which had no geometric losses with distance from the source, the shock wave would be transmitted into the water with no loss in peak pressure even at great depths.

During the course of these experiments, data were obtained in air at four different locations with respect to the flight path. Figure 9 shows how the peak pressure varies with distance from the flight path. It is interesting to note that while the decrease in peak pressure is generally assumed to be $\Delta p \sim 1/(h/l)^{3/4}$ for Mach numbers less than 3, the decrease here is more like $\Delta p \sim 1/(h/l)$, steeper presumably because of the higher Mach number and accompanying higher shock strength. The primary reason for introducing this curve, however, is to compare air data and data taken under water when the distance from the flight path to water surface is constant and water depth is varied by moving the plate deeper (and consequently farther from the flight path). When these data, taken at three different locations, are plotted in Fig. 10 with the curve for air data, one finds that they fall on top of the line. This demonstrates clearly that the only parameter of importance to the magnitude of peak pressure under water is the distance at which it is measured from the flight path. The magnitude of the peak pressure of the shock wave is not affected by the depth of water through which it travels. The implication for full-scale considerations are obvious. Any aircraft producing an incident shock wave on a water surface traveling at a speed greater than $M = 4.4$ will produce a shock wave in the water with no loss in its peak pressure due to water depth.‡ For aircraft at high altitude, the

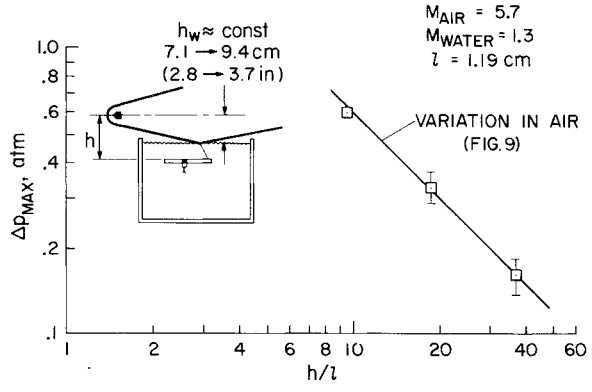

Fig. 10 Variation of peak pressure underwater with distance from flight path.

‡ The speed of the aircraft necessary to produce such an incident shock wave (i.e., which travels at speeds greater than the speed of sound in water) will depend on variations in local atmospheric conditions and flight-path angle.

incident shock wave at the surface can be considered essentially a planar wave and if the depth of interest in the ocean is small compared to the altitude of the airplane above the water, then the pressure at this depth is essentially the pressure experienced at the surface.

Concluding Remarks

An investigation of sonic-boom overpressures in water conducted by launching small models over water-filled tanks in a ballistic range yielded shadowgraph pictures and underwater pressure measurements that lead to the following conclusions.

1) Flights over water that produce an incident shock wave which travels along the surface of the water at speeds greater than the speed of sound in water ($M_{air} > 4.4$) produce shock waves in the water; the variation in peak pressure associated with the shock wave with distance from the flight path is not affected by water depth but behaves exactly as it does in air.

2) If the speed of the incident wave is less than $M = 4.4$, only sound waves are produced under water and the peak pressure decays rapidly with depth and is well predicted by theory.

Results of the present study infer that these conclusions may be applicable (under certain conditions) to full-scale flight; any extrapolation, however, can only be confirmed by full-scale flight tests.

References

[1] Sawyers, K. N., "Underwater Sound Pressure from Sonic Booms," *Journal of the Acoustical Society of America,* Vol. 44, No. 2, 1968, pp. 523–524.

[2] Cook, R. K., "Penetration of a Sonic Boom into Water," *Journal of the Acoustical Society of America,* Vol. 47, No. 5 (Pt. 2), 1970, pp. 1430–1436.

[3] Waters, J. F. and Glass, R. E., "Penetration of Sonic Boom Energy into the Ocean: An Experimental Simulation," HRC-TR-288, June 1970, Hydrospace Research Corp., Rockville, Md.

[4] Urich, R. J., "Sonic Booms in the Sea," NOLTR 71-30, Feb. 1971.

[5] Malcolm, G. N. and Intrieri, P. F., "Ballistic Range Investigation of Sonic-Boom Overpressures in Water," AIAA Paper 72-654, Boston, Mass., 1972.

[6] Wilkins, M. E., "Sonic Boom Effect on Fish—Observations," TM X-62,163, May 1972, NASA.

[7] Whitham, G. B., "The Flow Pattern of a Supersonic Projectile," *Communications in Pure and Applied Mathematics,* Vol. V, No. 3, Aug. 1952, pp. 301–348.

[8] Brekhovskikh, L. M., *Waves in Layered Media,* Academic Press, New York, 1960, pp. 15–25.

[9] *Physics of Sound in the Sea,* NAVMAT p-9675, 1969, U.S. Navy, pp. 27–28.